



ON THE SIGNIFICANCE OF ANTIRESONANCE FREQUENCIES IN EXPERIMENTAL STRUCTURAL ANALYSIS

F. WAHL AND G. SCHMIDT

*Institut für Mechanik, Otto-von-Guericke-Universität, Universitätsplatz 2,
39106 Magdeburg, Germany*

AND

L. FORRAI

*Department of Mechanics, University of Miskolc, 3515 Miskolc-Egyetemváros,
Hungary*

(Received 25 November 1997, and in final form 17 June 1998)

The resonance–antiresonance behaviour of frequency response functions (FRFs) for linear lightly damped structures is discussed. The focus is on the significance of antiresonances in experimental structural analysis. Consideration of the relationship between the resonance–antiresonance behaviour and structural modification gives a physical interpretation of the phenomenon of antiresonances. It shows that the antiresonance frequencies of measured FRFs provide useful information on the dynamic properties of a test structure. So, from the experimentally determined antiresonance frequencies of a structure under arbitrary boundary conditions, it is possible to determine the resonance frequencies of the structure under ideal boundary conditions which are impossible to achieve in laboratory tests. The results presented serve as a basis for further experimental research in fields such as identification, updating finite element models, and location of structural faults.

© 1999 Academic Press

1. INTRODUCTION

In experimental structural analysis, frequency response functions (FRFs) play a dominant role. They provide the engineer with important information on the dynamic behaviour of the structure under consideration and at the same time they serve as a reference for most parameter estimation procedures. Here special attention is directed to the driving point FRFs where the response co-ordinate and the excitation co-ordinate are identical.

The investigations here are confined to linear, reciprocal, mass and stiffness controlled systems: i.e., to structures which, because of light damping and low modal density, exhibit a pronounced resonance–antiresonance behaviour. In reference [1] it has been explained that for such systems the driving point FRF

plots are characterized by a successive change in the resonances and antiresonances.

Figure 1 shows the measured driving point FRF plots for different structures: the FRF for a simple structure (cantilever beam), and the FRF for a complex structure (12-cylinder engine block). As can be seen there is a successive change in the resonances and antiresonances for both structures, regardless of the complexity of structures. If for a measured driving point FRF this change is not pronounced, then either the measurement is erroneous or the structure cannot be described by the assumed model.

The purpose of this paper is to direct attention to the significance of antiresonance frequencies by using experimentally determined FRFs. It is clear that the resonance frequencies represent mathematically the zeros of the denominator polynomial, whereas the antiresonance frequencies are the zeros of the numerator polynomial. From this, however, the physical explanation of the phenomenon of antiresonances cannot be easily derived. While in dynamics of machines the antiresonance behaviour of discrete systems has been known for a long time by the name “vibration absorption”, in experimental structural analysis there have been only few works which deal with the phenomenon of antiresonances.

In reference [2] the theoretical background of antiresonances in terms of modes and vibratory waves has been discussed and the importance of antiresonances in future research (health monitoring and localization of damages) has been stressed. In addition, the experimental investigations of antiresonances and the corresponding mode shapes of a bridge have also been described. The theoretical and experimental results of the resonance–antiresonance behaviour of a cantilever beam have been presented in reference [3]. It has been shown, for instance, that the antiresonance frequencies of the beam are equal to the resonance frequencies of the system in which a stiff restraint of displacement is added to the excitation point.

In this paper, it will be shown what type of information can be acquired from the antiresonance frequencies by using the driving point FRFs, and what the importance of this information is for experimental structural analysis. The investigations are based on the close relationship between the structural modification and the resonance–antiresonance behaviour of elastic structures by which it is possible to give a simple physical interpretation of the antiresonance

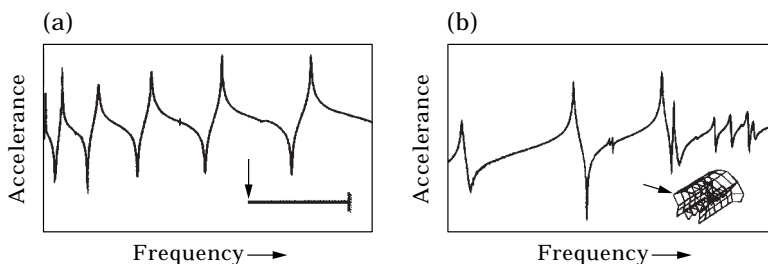


Figure 1. Examples of measured driving point FRFs. (a) Cantilever beam; (b) 12-cylinder engine block.

behaviour. Both single reference input systems and multiple reference input systems will be discussed.

As a significant result, it will be shown that the antiresonance frequencies can be interpreted as the resonance frequencies of the system fixed at the excitation points in the excitation directions. Thus, from the measurements on a freely-supported structure or on a structure without precisely defined boundary conditions, it is possible to determine the eigenfrequencies of the structure with precisely defined boundary conditions. The latter has been verified by experimental investigations for a rectangular plate. The consequences of the results for experimental research, as well as possible applications, will also be presented.

2. STRUCTURAL MODIFICATION AND RESONANCE–ANTIRESONANCE BEHAVIOUR

2.1. PRELIMINARY REMARKS

To simplify the following theoretical considerations, undamped structures are assumed. The experimental investigations have shown that the results obtained from undamped structures can also be validated without restrictions for very lightly damped structures (damping loss factor is typically less than 0.01).

2.2. SINGLE REFERENCE INPUT

Consider a general structure driven by a force $f_k(t)$ at a single measurement DOF k with displacement response $x_l(t)$ at any other measurement DOF l . After using the Fourier transforms of $f_k(t)$ and $x_l(t)$, the FRF $H_{lk}(\omega)$ can be written in the form

$$H_{lk}(\omega) = X_l(\omega)/F_k(\omega), \quad (1)$$

or, after rewriting,

$$X_l(\omega) = H_{lk}(\omega)F_k(\omega), \quad (2)$$

where $X_l(\omega)$ and $F_k(\omega)$ are the Fourier transforms of $x_l(t)$ and $f_k(t)$, respectively, and ω is the excitation frequency. The FRF $H_{lk}(\omega)$ is known as the receptance.

For undamped or lightly damped structures, the magnitude of the FRF $H_{lk}(\omega)$ is essentially characterized by a resonance–antiresonance pattern in the frequency domain. When comparing the FRFs for different response DOFs, one sees that the resonance frequencies as global quantities are the same for all the FRFs, whereas the antiresonance frequencies and their number also depend on the response DOF. As a rule of thumb, it can be stated that by increasing the distance between the excitation DOF and the response DOF the number of antiresonance ranges decreases (see example reference [1]). The resonances and antiresonances alternate continuously only for those FRFs where the excitation DOF and response DOF coincide.

This paper deals with the problem of what supplementary information can be obtained from the knowledge of antiresonances by using measured FRFs. To answer this problem, use is made of the close relationship between the resonance–antiresonance behaviour and the structural modification. To this end,

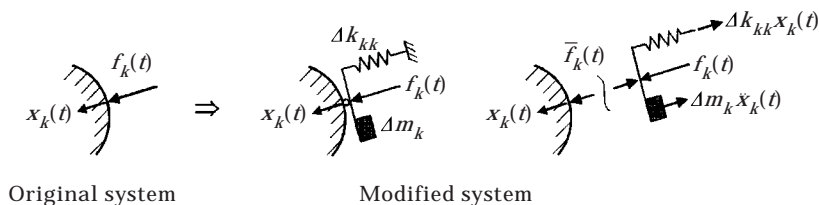


Figure 2. Mass and stiffness modifications at excitation DOF k .

the structure is modified by adding a mass Δm_k and/or a stiffness Δk_{kk} to the excitation point in the excitation direction (see Figure 2) and the behaviour of the changed FRF $\bar{H}_{\ell k}(\omega)$ is observed. For the modified structure, one has

$$X_{\ell}(\omega) = \bar{H}_{\ell k}(\omega)F_k(\omega), \quad (3)$$

and for the original structure, one now obtains the equation

$$X_{\ell}(\omega) = H_{\ell k}(\omega)\bar{F}_k(\omega). \quad (4)$$

The reduced excitation force $\bar{f}_k(\omega)$ (see Figure 2) can be written as

$$\bar{f}_k(t) = f_k(t) - [\Delta m_k \ddot{x}_k(t) + \Delta k_{kk} x_k(t)], \quad (5)$$

which after using the Fourier transforms becomes

$$\bar{F}_k(\omega) = F_k(\omega) - [-\omega^2 \Delta m_k X_k(\omega) + \Delta k_{kk} X_k(\omega)]. \quad (6)$$

By substituting equation (6) into equation (4) and introducing the relations

$$H_{\ell k}(\omega)X_k(\omega) = \frac{X_{\ell}(\omega)}{\bar{F}_k(\omega)}X_k(\omega) = \frac{X_k(\omega)}{\bar{F}_k(\omega)}X_{\ell}(\omega) = H_{kk}(\omega)X_{\ell}(\omega), \quad (7)$$

the modified FRF can be written as

$$\bar{H}_{\ell k}(\omega) = \frac{H_{\ell k}(\omega)}{1 + H_{kk}(\omega)\Delta b_{kk}(\omega)}, \quad (8)$$

where

$$\Delta b_{kk}(\omega) = (-\omega^2 \Delta m_k + \Delta k_{kk}). \quad (9)$$

From the equation (8) one can derive the basic relationships between the structure modification $\Delta b_{kk}(\omega)$ and the resonance–antiresonance behaviour of the structure. It will be seen that for any modification $\Delta b_{kk}(\omega)$ the zeros of the modified FRF $\bar{H}_{\ell k}(\omega)$ must coincide with those of the original FRF $H_{\ell k}(\omega)$. Since for undamped or lightly damped structures the zeros represent the antiresonance frequencies, the following theorem holds true: the antiresonance frequencies of an arbitrary FRF do not change if any mass or any stiffness is added to the structure at the excitation point in the excitation direction.

By applying the reciprocity principle for the structure's behaviour ($H_{\ell k}(\omega) = H_{k\ell}(\omega)$), the following conclusion can be drawn: the antiresonance frequencies of an arbitrary FRF do not change if any mass or any stiffness is added to the structure at the response point in the response direction.

Before considering the importance of these theorems for experimental structural analysis, first the resonance behaviour of the modified structure must be investigated. To do this, use is made of the driving point FRF, in which the excitation DOF and the response DOF are the same. From equation (8) one obtains

$$\bar{H}_{kk}(\omega) = \frac{H_{kk}(\omega)}{1 + H_{kk}(\omega)\Delta b_{kk}(\omega)}. \tag{10}$$

The resonance frequencies of the modified structure are determined from the zeros of the denominator of equation (10), i.e. from the equation

$$-1/\Delta b_{kk}(\omega) = H_{kk}(\omega). \tag{11}$$

Equation (11) is derived in the reanalyses techniques of undamped structures [4] and in the structural modification theory for desired pole shifting of damped systems [5]. Equation (11) has a simple graphical interpretation. To simplify our analysis, a mass modification is introduced. With equation (9) one then obtains from equation (11)

$$1/\Delta m_k = \omega^2 H_{kk}(\omega) = -H_{kk}^a(\omega). \tag{12}$$

The right side of this equation is known as the acceleration (or inertance) $H_{kk}^a(\omega)$, which is defined as the ratio of the vibration acceleration to the excitation force and can be directly measured. For graphical representation, it is practical to rewrite equation (12) with the aid of a logarithmic decibel scale:

$$20 \lg \left| \frac{1}{\Delta m_k} \right| = 20 \lg |H_{kk}^a(\omega)| \quad (\text{dB}). \tag{13}$$

Equation (13) describes the shifts in resonance frequencies due to an additional mass applied at the excitation DOF of the structure. The right side of equation (13) represents the measured driving point FRF (accelerance). The points of intersection of the accelerance curve with the horizontal line $|1/\Delta m_k|$ give the resonance frequencies of the modified structure.

Before studying the role of antiresonances in detail, one can first elucidate the results presented thus far by using the 3-DOF vibratory structure shown in Figure 3. The circled numbers indicate the simulated measurement DOFs.

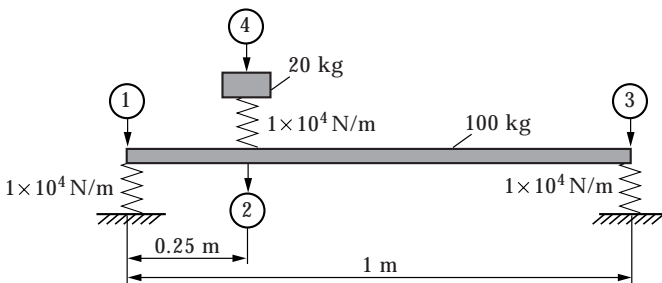


Figure 3. 3-DOF vibratory structure with four measurement DOFs.

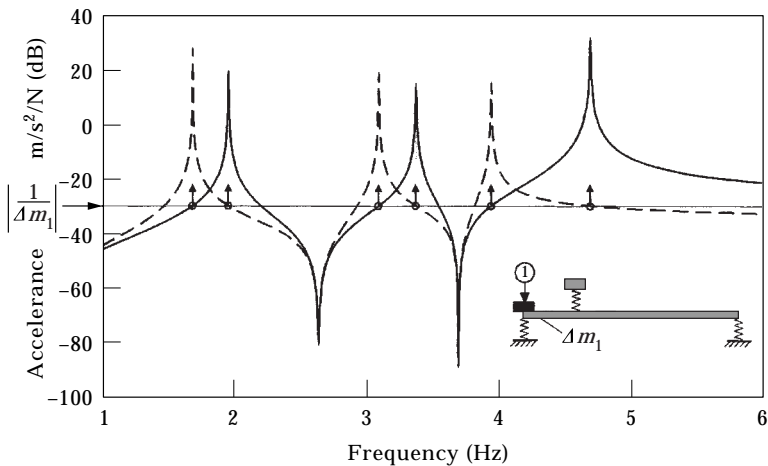


Figure 4. Mass modification and resonance shifts. —, FRF $H_{11}^a(\omega)$ for the original structure; ---, FRF $\bar{H}_{11}^a(\omega)$ for the modified structure; $\Delta m_1 = 31.6$ kg (30 dB).

Figure 4 shows the driving point FRF $H_{11}^a(\omega)$ for the original structure and the driving point FRF $\bar{H}_{11}^a(\omega)$ for the structure modified by the additional mass Δm_1 . It can be seen that the antiresonance frequencies do not change due to the additional mass. By virtue of equation (13), the shifts in resonance frequencies are determined from the points of intersection of the horizontal line $|1/\Delta m_1|$ with the accelerance $|H_{11}^a(\omega)|$. This procedure is reversible. If the mass Δm_1 is removed, then the resonances corresponding to the points of intersection with the horizontal line $|1/\Delta m_1|$ will be shifted again to the right into their initial positions.

The driving point FRFs $H_{11}^a(\omega)$ for different values of the additional mass Δm_1 are shown in Figure 5. By increasing the additional mass, the resonances are shifted to the left in the direction of the antiresonance frequencies. It is seen that all the antiresonances are unchanged. The shifts of resonance frequencies beyond

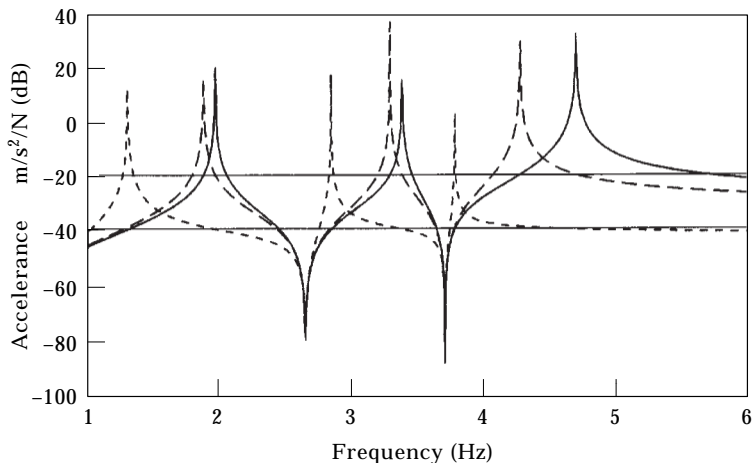


Figure 5. FRFs $\bar{H}_{11}^a(\omega)$ with different additional masses. —, Original; ---, $\Delta m_1 = 10$ kg (20 dB); - · - ·, $\Delta m_1 = 100$ kg (40 dB).

the antiresonance frequencies are not possible. When the mass becomes infinite ($\Delta m_1 \rightarrow \infty$), the resonances “fall into the antiresonances”. This limited case can be interpreted physically by the fact that, when increasing the additional mass Δm_1 , the nodes of the mode shapes approach the excitation point and in the limit case they lie in the excitation point and fix the structure in the excitation direction.

Thus, the condition for determination of the resonance frequencies of a structure, whose excitation DOF is held fixed, can be obtained from equation (12) as

$$H_{kk}(\omega) = 0. \quad (14)$$

Since the zeros of the driving point FRF $H_{kk}(\omega)$ provide the antiresonance frequencies, the following conclusion can be drawn: the antiresonance frequencies for an arbitrary driving point FRF are identical with the resonance frequencies of the structure that is fixed at the excitation point in the excitation direction.

It is interesting to note that in reference [6], an equation is derived for calculating the eigenfrequencies of a N -DOF system under constraint. This equation is

$$\sum_{r=1}^N \frac{a_r}{(-\omega^2 + \omega_r^2)} = 0, \quad (15)$$

which is identical to equation (14) in the modal domain.

A further generalization of single reference input systems is possible by considering the stiffness modification Δk_{kl} between the two measurement DOFs k and l with the same direction. By forming the “relative” driving point FRF (see for example reference [5])

$$\Delta H_{kl}(\omega) = H_{kk}(\omega) - 2H_{kl}(\omega) + H_{ll}(\omega), \quad (16)$$

the corresponding FRF for the modified structure is obtained from a formula analogous to equation (10):

$$\Delta \bar{H}_{kl}(\omega) = \frac{\Delta H_{kl}(\omega)}{1 + \Delta H_{kl}(\omega) \Delta k_{kl}}. \quad (17)$$

It can be shown that the function $\Delta H_{kl}(\omega)$ represents the same resonance–antiresonance behaviour as the customary driving point FRF. Therefore, the same theorems also hold true. For these, the following apply: the antiresonance frequencies of an arbitrary FRF $\Delta H_{kl}(\omega)$ do not change if any stiffness modification is made between the measurement DOFs k and l ; the antiresonance frequencies of an arbitrary FRF $\Delta H_{kl}(\omega)$ are identical to the resonance frequencies of the structure, in which the structure is coupled rigidly between the measurement DOFs k and l .

Figure 6 shows the FRFs $\Delta H_{24}(\omega)$ and $\Delta \bar{H}_{24}(\omega)$ for the 3-DOF vibratory structure. The modification Δk_{24} shifts the resonances to the right, whereas the antiresonances remain unaffected. The antiresonance frequencies can be interpreted as the resonance frequencies for the structure coupled rigidly between the measurement DOFs 2 and 4.

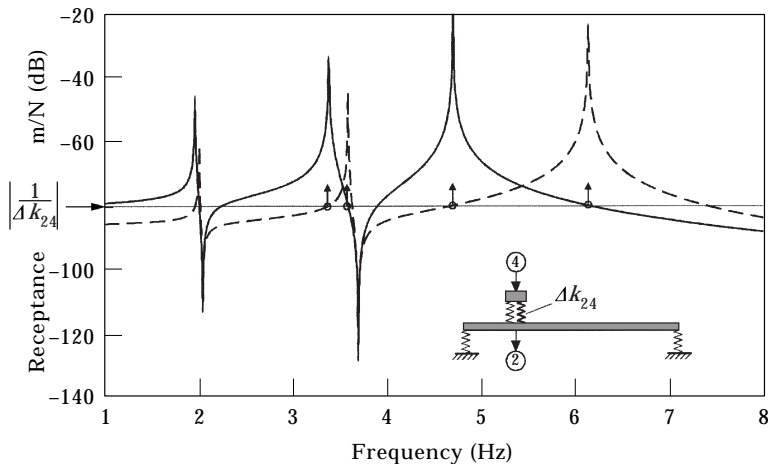


Figure 6. Relative stiffness modification and resonance shifts. —, FRF $\Delta H_{24}(\omega)$ for the original structure; ---, FRF $\Delta \bar{H}_{24}(\omega)$ with $\Delta k_{24} = 10\,000$ N/m (80 dB).

2.3. MULTIPLE REFERENCE INPUT

If the structure considered is excited at multiple excitation DOFs, the relationships between the structure modification and the resonance–antiresonance behaviour can be described in a similar manner as in the case of single reference input systems. Assuming n excitation DOFs and n response DOFs, one obtains

$$\mathbf{X}(\omega) = \mathbf{H}(\omega)\mathbf{F}(\omega), \tag{18}$$

where $\mathbf{F}(\omega)_{(1 \times n)}$ is the vector of excitation forces, $\mathbf{X}(\omega)_{(1 \times n)}$ the vector of displacements, and $\mathbf{H}(\omega)_{(n \times n)}$ the FRF matrix. Let us further assume that $\mathbf{H}(\omega)$ is a full rank matrix.

Proceeding in the same manner as in the case of single input reference systems, one obtains the vector of the reduced exciting forces in the form

$$\bar{\mathbf{F}}(\omega) = \mathbf{F}(\omega) - \Delta \mathbf{B}(\omega)\mathbf{X}(\omega), \tag{19}$$

with

$$\Delta \mathbf{B}(\omega) = (-\omega^2 \Delta \mathbf{M} + \Delta \mathbf{K}). \tag{20}$$

Let the matrices $\Delta \mathbf{M}$ and $\Delta \mathbf{K}$ be diagonal matrices whose elements describe the modifications at the n excitation DOFs. For the modified structure, one now obtains the equation for the FRF matrix:

$$\bar{\mathbf{H}}(\omega) = [\mathbf{I} + \mathbf{H}(\omega)\Delta \mathbf{B}(\omega)]^{-1}\mathbf{H}(\omega). \tag{21}$$

Taking the eigenvalue decomposition of the FRF matrix $\mathbf{H}(\omega)$ at each spectral line (simple eigenvalues are assumed) one has

$$\mathbf{T}^T(\omega)\mathbf{H}(\omega)\mathbf{T}(\omega) = \mathbf{\Lambda}(\omega), \tag{22}$$

where $\mathbf{T}(\omega)$ is the matrix of the orthonormalized eigenvectors and $\mathbf{\Lambda}(\omega)$ is the diagonal eigenvalue matrix.

If one assumes that the modifications $\Delta b_{kk}(\omega)$, $k = 1, 2, \dots, n$, at all excitations DOFs are identical to $\Delta b(\omega)$, one obtains

$$\Delta \mathbf{B}(\omega) = \Delta b(\omega) \mathbf{I}, \quad (23)$$

and the eigenvalue decomposition of the modified FRF matrix is given by

$$\mathbf{T}^T(\omega) \bar{\mathbf{H}}(\omega) \mathbf{T}(\omega) = \bar{\Lambda}(\omega), \quad (24)$$

with

$$\bar{\Lambda}(\omega) = [\mathbf{I} + \Lambda(\omega) \Delta b(\omega)]^{-1} \Lambda(\omega). \quad (25)$$

From equation (25) one obtains the r th eigenvalue as

$$\bar{\Lambda}_r(\omega) = \frac{\Lambda_r(\omega)}{1 + \Lambda_r(\omega) \Delta b(\omega)}. \quad (26)$$

By comparing equations (26) and (10), it can be seen that the same relationships are valid for the eigenvalues of the FRF matrix $\mathbf{H}(\omega)$ as in the case of single reference input systems. Therefore, the conclusions drawn for single reference input systems can be validated directly for multiple reference input systems: the antiresonance frequencies of the eigenvalues $\Lambda_r(\omega)$ do not change if any mass or any stiffness is added to the structure at all n excitation points in the corresponding excitation directions; the antiresonance frequencies of the eigenvalues are identical with the resonance frequencies of the structure that is fixed at all n excitation points in the corresponding excitation directions.

Since arbitrary structural modifications at the excitation DOFs must give identical resonance frequencies of the structure fixed at all n excitation points in the corresponding excitation directions, the assumption (23) can be omitted and it follows that the antiresonance frequencies of the eigenvalues $\Lambda_r(\omega)$ do not change due to arbitrary mass or stiffness modifications at k excitation points ($k = 1, 2, \dots, m, m \leq n$) in the corresponding excitation directions. This theorem is important for testing structures because the size of the shakers and transducers need not to be identical.

The results are elucidated in the example of the 3-DOF vibratory structure shown in Figure 3. Let the excitation DOFs be points 1 and 3. Two identical masses Δm are added to these points. The eigenvalues $\Lambda_1^a(\omega)$ and $\Lambda_2^a(\omega)$ of the accelerance matrix

$$\mathbf{H}^a(\omega) = \begin{bmatrix} H_{11}^a(\omega) & H_{13}^a(\omega) \\ H_{31}^a(\omega) & H_{33}^a(\omega) \end{bmatrix}, \quad (27)$$

as well as the eigenvalues $\bar{\Lambda}_1^a(\omega)$ and $\bar{\Lambda}_2^a(\omega)$ of the modified FRF matrix $\bar{\mathbf{H}}^a(\omega)$ are shown in Figure 7. It can be seen that the resonance–antiresonance behaviour of the eigenvalues is similar to the behaviour of the FRFs for single reference input systems. The antiresonance frequency shown in Figure 7 is identical with the

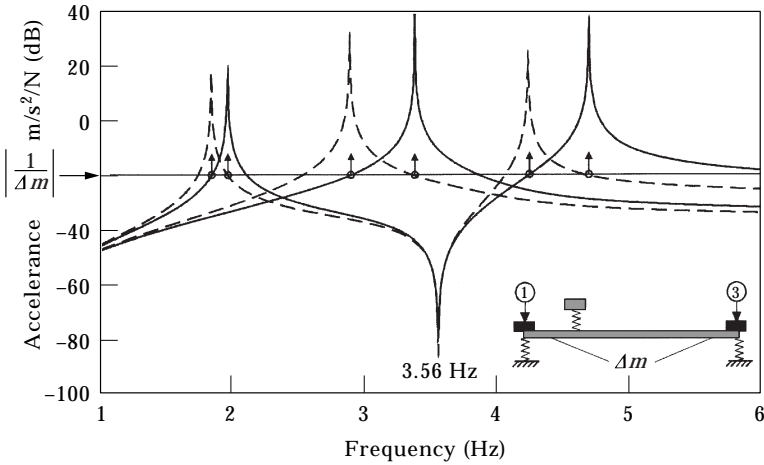


Figure 7. Mass modification and resonance shifts. —, Eigenvalues $A_1^q(\omega)$ and $A_2^q(\omega)$ for the original structure; ---, eigenvalues $\bar{A}_1^q(\omega)$ and $\bar{A}_2^q(\omega)$ for the modified structure; $\Delta m = 10$ kg (20 dB).

resonance frequency of the structure that is fixed at points 1 and 3. There remains a single DOF system with the eigenfrequency (see Figure 3)

$$f = \frac{1}{2\pi} \sqrt{\frac{10000}{20}} \text{ Hz} = 3.56 \text{ Hz.}$$

The significance of antiresonance frequencies in experimental structural analysis can be explained by another example for a continuous system. Figure 8 shows the plot for the eigenvalues of the accelerance matrix using the excitation points shown (at the top of the figure). The resonance frequencies of the eigenvalues $A_1^q(\omega)$ and $A_2^q(\omega)$ are the eigenfrequencies of the original system and the antiresonance frequencies of the eigenvalues give eigenfrequencies of the clamped beam (at the bottom of the figure).

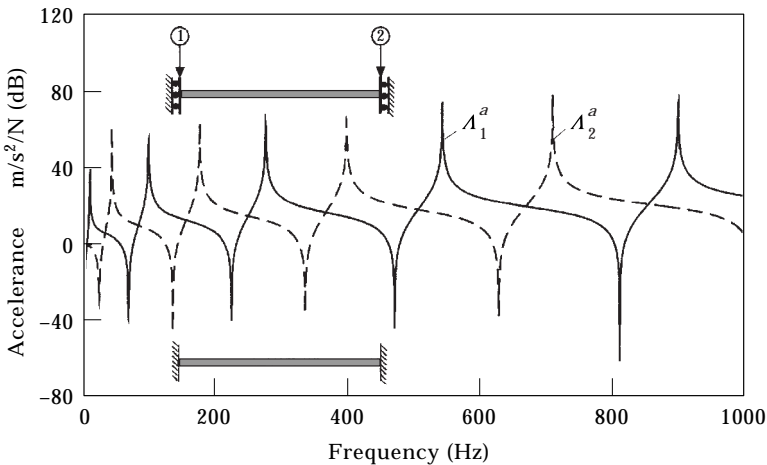


Figure 8. Significance of antiresonance frequencies for the eigenvalues $A_1^q(\omega)$ and $A_2^q(\omega)$. Beam parameters: $L = 1$ m; $\rho aL = 2$ kg; $EI = 100$ Nm².

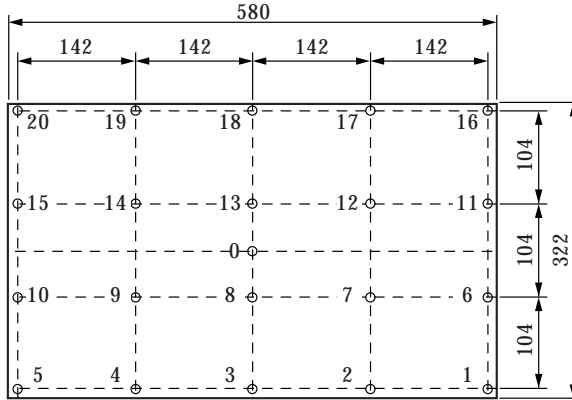


Figure 9. Test structure with lay-out of the test points. Dimensions in mm.

From the properties of antiresonances presented here important conclusions can be drawn for experimental structural analysis. By using the FRF measurements of structures supported arbitrarily it is possible to determine the eigenfrequencies of structures in ideal support conditions that are impossible to achieve in laboratory tests.

3. EXPERIMENTAL RESULTS

To verify the theoretical results and the numerical examples, experimental investigations were performed. As a test structure, a rectangular steel plate ($580 \times 332 \times 4.1$) mm was used. The plate with the lay-out of the testpoints is shown in Figure 9. The plate was supported by rubber cables at points 16 and 20 so that the eigenfrequencies of rigid body motions were found below the first eigenfrequency of the elastic deformations (free-free boundary condition). For the measurements of the FRFs and for the modal analysis, the LMS CADA-X software was used. An impact hammer was employed as an exciter. The excitations and the measurements of vibration accelerations were carried out normal to the plate surface.

In the first test, the relationships between the modification and the resonance-antiresonance behaviour presented for single reference input systems were revised. For this purpose, the driving point FRF for the centre of the plate (point 0) was measured in the frequency range up to 2500 Hz. To avoid rotations of the added mass and to ensure by this a pure mass modification in the excitation direction, the point 0 was chosen. Figure 10 shows the plots of $H_{0,0}^a(\omega)$ for the original structure and $\bar{H}_{0,0}^a(\omega)$ for the structure modified by the additional mass Δm_0 . The results confirm equation (13) concerning the shifts in resonance frequencies, and at the same time they show that the antiresonance frequencies are not shifted due to modifications at the excitation point. The antiresonance frequencies shown in Figure 10 can be interpreted as the eigenfrequencies of the plate fixed at point 0.

The results for multiple reference input systems were verified with the aid of another test. The softly suspended plate was excited at three points: 4, 11 and 19.

The complete FRF matrix $\mathbf{H}^a(\omega)$ was measured in the frequency range up to 250 Hz. After modal identification, the complex eigenvalues of the FRF matrix $\mathbf{H}^a(\omega)$ were calculated for each frequency line. Figure 11(a) shows the eigenvalue curves $A_1^a(\omega)$, $A_2^a(\omega)$ and $A_3^a(\omega)$ of the FRF matrix.

To test the antiresonance frequencies, the plate was subsequently supported horizontally by pointed edges at points 4, 11, and 19. The FRF $H_{1,1}^a(\omega)$ of the plate supported in this manner is shown in Figure 11(b). As can be seen there is a good agreement between the antiresonance frequencies of the eigenvalues for the original plate and the resonance frequencies for the plate supported at the excitation points. The frequency values are tabulated in Table 1 (columns 1 and 2). For further verification of the results, FE-calculations were carried out. The results are shown in Table 1, column 3.

In the case of the supported plate, it was clearly not possible to measure the expected eigenfrequency of 78.9 Hz (third antiresonance). The reason for this lies in the fact that the plate was supported on edges against its own weight. To eliminate the disturbing effects, the two-sided support conditions were not employed. On account of the unfavourable mode shape at 78.9 Hz, the weight of the plate was insufficient to ensure the appropriate supporting conditions, through which it was not possible for the corresponding mode shape to develop.

4. APPLICATIONS IN EXPERIMENTAL STRUCTURAL ANALYSIS

The application of the results obtained from the antiresonance behaviour of elastic structures is of importance in the following fields of experimental structural analysis.

1. Experimental modal analysis. The user of experimental modal analysis must pay attention to the fact that the antiresonance ranges should also be correctly contained in the regenerated FRF curves, otherwise the identified modal model

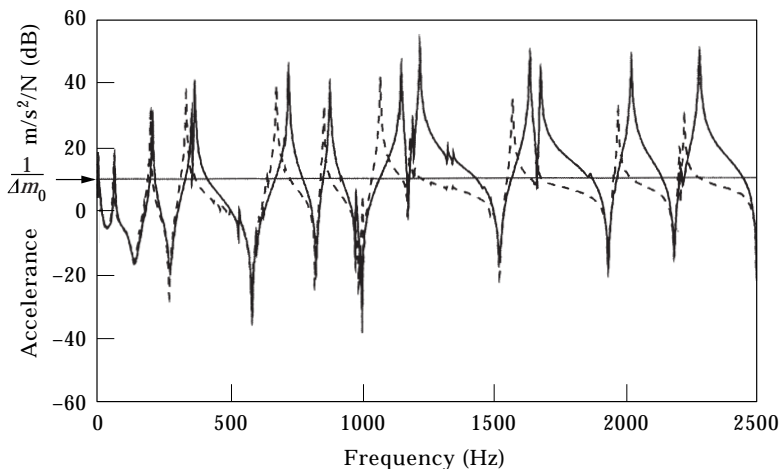


Figure 10. Measured driving point FRFs for the plate. —, FRF $H_{0,0}^a(\omega)$ for the original plate; ---, FRF $\bar{H}_{0,0}^a(\omega)$ for the modified plate; $\Delta m_0 = 0.316$ kg (-10 dB).

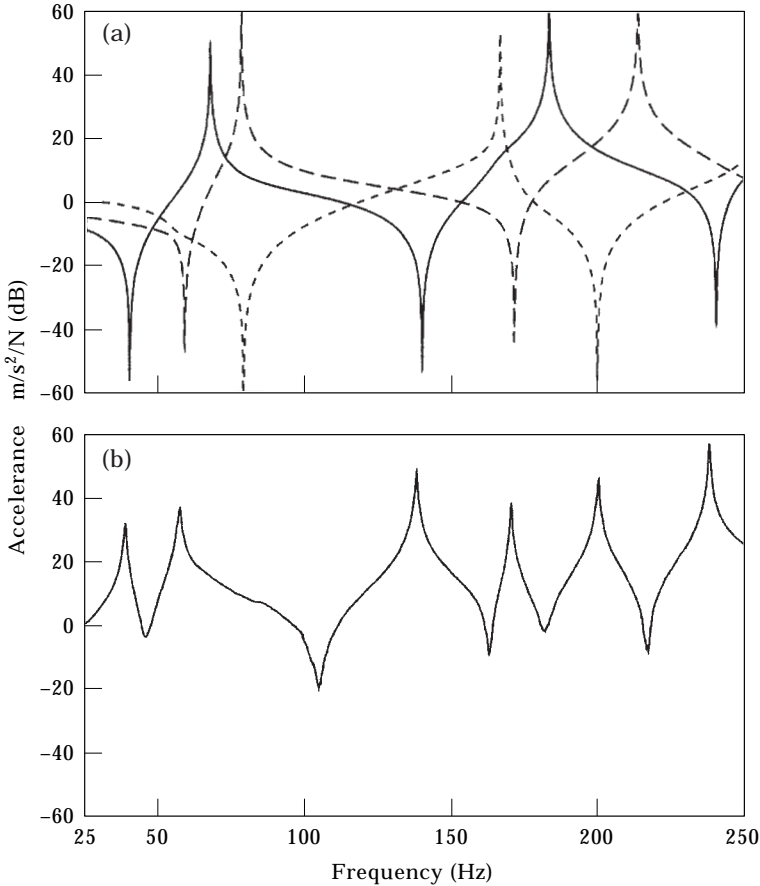


Figure 11. (a) Eigenvalues for the plate in free-free boundary condition (measurement points 4, 11 and 19). —, $A_1^g(\omega)$; ---, $A_2^g(\omega)$; -·-, $A_3^g(\omega)$. (b) Measured FRF $H_{i,1}^g(\omega)$ for the plate supported at points 4, 11 and 19.

may be erroneous in other boundary conditions (e.g., support at the excitation points).

2. Updating finite element models. By using experiments, the eigenfrequencies of a test structure can easily be measured for different ideal boundary conditions. Since it is possible to virtually fix the structure to be tested at each point and in each measurement direction (provided that the measurement of the driving point FRF is practically possible), updating can be carried out step-by-step using the separation of complicated ranges.

3. Identification. In the case of parameter identification, a complicated model can be simplified by fixing substructures (see Figure 7). When changing the boundary conditions for the test we may obtain more information concerning the indirect identification of parameters.

4. Location of structural faults. Any modification of structures (faults) causes shifts in the resonance frequencies as well as in the antiresonance frequencies. The consideration of antiresonance frequencies provides more information and can be a useful indicator for the location of structural faults. If the resonance frequencies

of a structure change for a given excitation DOF at a response DOF, while the antiresonance frequencies remain unchanged, then a modification of the structure (structural fault) at this response DOF can be predicted.

5. SUMMARY AND CONCLUSIONS

In this paper, the significance of antiresonances in experimental structural analysis has been discussed. Linear systems with light damping (mass stiffness controlled systems) are assumed. The consideration of the relationship between structural modification and resonance–antiresonance behaviour provides a simple physical interpretation of the antiresonance frequencies. It is shown that for single input reference systems the antiresonance frequencies of an arbitrary driving point FRF are identical with the resonance frequencies of the system fixed at the excitation point in the excitation direction. For multiple input reference systems, fully analogous theorems can be derived if the driving point FRFs are replaced by the eigenvalues of the corresponding FRF matrix. These eigenvalues exhibit a similar resonance–antiresonance behaviour as the driving point FRFs for single input reference systems.

From the presented properties of antiresonances, important conclusions can be drawn for experimental structural analysis: from the FRF measurements of structures supported arbitrarily, it is possible to determine the eigenfrequencies of structures under ideal boundary conditions which are impossible to achieve in laboratory tests. This leads to future applications in different fields of structural analysis such as identification and location of structural faults. However, the results presented above also indicate that in the modal parameter estimation procedures particular attention should be paid to the fact that the regenerated FRF curves describe adequately the antiresonance ranges too.

TABLE 1

Comparison between the antiresonance frequencies of the eigenvalues for the plate in free–free boundary conditions and the eigenfrequencies of the plate supported at point 4, 11 and 19 (data in Hz).

No.	Antiresonance frequencies of eigenvalues of the free–free plate	Eigenfrequencies: measurement supported plate	Eigenfrequencies: FEM supported plate
1	40.2	39.5	41.05
2	58.7	57.9	57.88
3	78.9	–	77.35
4	139.8	138.5	143.9
5	171.3	170.7	173.8
6	199.6	200.3	203.0
7	240.1	238.2	242.6

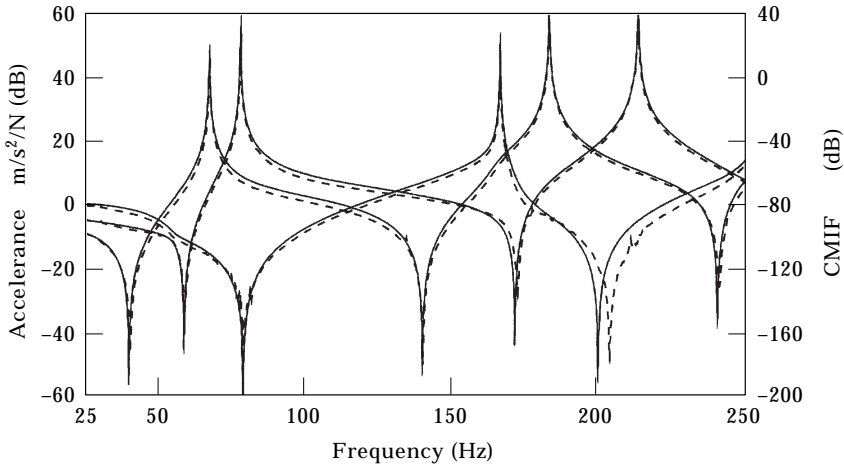


Figure 12. Eigenvalues $A_r^a(\omega)$ and Complex Mode Indicator Functions $CMIF$, for the plate in free-free boundary condition (measurement points 4, 11 and 19). —, $A_r^a(\omega)$, $A_s^s(\omega)$, $A_s^s(\omega)$ after modal identification; ---, $CMIF_1$, $CMIF_2$, $CMIF_3$ calculated from the measured FRF matrix.

Some problems encountered in practice are as follows.

In calculating the eigenvalues of complex FRF matrices, which are based on measurements, numerical problems may occur in the range of antiresonances because measurements will become noise contaminated when the response signal tends to zero. An additional difficulty arises if the resonances and antiresonances are closely spaced. Small phase errors may lead to large distortions in the antiresonance ranges. For these reasons, the direct calculation of the eigenvalues of the FRF matrices is useful only for a small number of degrees of freedom. For larger FRF matrices, it is necessary to perform a modal identification before calculating the eigenvalues. In this case, when using modal analysis, particular attention must be paid to the correct determination of the residual terms (out of range modes) because these greatly influence the position of the antiresonances. An appropriate solution of this problem seems to be a new approach for dynamic residual compensation found in reference [7].

An alternative method for calculating the antiresonance frequencies from measured FRF matrices without modal identification is presented by the Complex Mode Indicator Function (CMIF). The CMIFs are defined as the eigenvalues solved from the normal FRF matrix ($\mathbf{H}^H(\omega) \cdot \mathbf{H}(\omega)$) at each spectral line and are expressed using singular value decomposition. For lightly damped systems the CMIFs of the FRF matrix exhibit nearly the same resonance-antiresonance behaviour as the eigenvalues themselves. The calculation of the CMIFs from FRF matrices has proved to be a stable algorithm, moreover implemented as standard software in modal analysis systems [8].

Figure 12 shows a comparison between the eigenvalues of the FRF matrix after modal identification (see Figure 11) and the corresponding CMIFs. Obviously, the curves of the CMIFs are very close to the eigenvalues. Only near the 200-Hz frequency line does a difference of nearly 3 Hz occur. The previously existing

conditions allow the conclusion that the CMIFs demonstrate the most correct value of the antiresonance frequency. But a final evaluation will be possible only after future research.

REFERENCES

1. D. J. EWINS 1984 *Modal Testing: Theory and Practice*. New York: Wiley.
2. S. J. PIETRZKO 1996 *Proceedings of the 21th International Conference on Noise and Vibration Engineering ISMA21*, Volume III, 1327–1335. Resonance and antiresonance dynamic behaviour of large mechanical systems.
3. F. Q. WANG, X. L. HAN and Y. Z. GUO 1996 *Journal of Vibration and Acoustics* **118**, 663–667. Analysis of characteristics of pseudo-resonance and anti-resonance.
4. V. W. SNYDER 1986 *The International Journal of Analytical and Experimental Modal Analysis* **1**, 45–52. Structural modification and modal analysis—a survey.
5. F. WAHL and R. JUNGLUTH 1995 *Zeitschrift für Angewandte Mathematik und Mechanik*, **75**, SI, S305–S306. Desired eigenvalue modification using incomplete modal information (in German).
6. R. E. D. BISHOP, G. M. L. GLADWELL and S. MICHAELSON 1965 *The Matrix Analysis of Vibration*. Cambridge: University Press.
7. M. L. M. DUARTE and D. J. EWINS 1996 *Proceedings of the Conference Identification in Engineering Systems, Swansea, UK*, 1277–1286. Experimental estimation of the high-frequency residual term based on two extra parameters.
8. LMS CADA-X USER MANUAL, Revision 3.4. Leuven, Belgium: LMS International.